Crystalline Silicon Solar Cell Engineering to Improve Fill Factor, Open Circuit Voltage, Short Circuit Current and Overall Cell Efficiency

Hadi Bashiri[1], Mohammad Azim Karami[2]*, and Shahram Mohammad Nejad[3]

Received: 2016-5-06 Accepted 2016-6-06

Abstract:

Design and optimization of a single crystalline silicon (c-Si) solar cell is performed to achieve the maximum light conversion efficiency. Various parameters such as doping concentration and thicknesses, and geometrical dimension of surface pyramids are studied. The inverted surface pyramid is used to increase the efficiency of the solar cell, and engineered oxide layer is used as the passivation and anti-reflect layer. Semi-analytic modeling of the output parameters of the solar cell, and numerical simulation for the structures are performed for the optimization. Fill factor (*FF*) of 85.4%, open circuit voltage (V_{OC}) of 761 *mV*, short circuit current density (J_{SC}) of 40.1 mA/cm^2 and the overall cell efficiency of 26.3% are achieved. The optimization procedure leads to 1.5% efficiency increase in compare with the similar works.

Index terms- silicon solar cell- efficiency- Ion implantation- Metal contact- Surface texturing

Silicon solar cell with mature processing properties such as standard process to implant both n- and p-type wells, the electrical band gap close to optimum value for maximum sun's light absorption, abundance of raw materials is the main candidate as a low-cost, high-efficiency photovoltaic module. The crystalline solar cell efficiency is improved up to 19.8% in multi-crystalline type, and 24.7% in mono-crystalline type [1-4]. Several efforts have been made to increase the efficiency of Si solar cells, such as the replacement of Al Back Side Field (BSF) with dielectric passivation in crystalline passivated emitter with rear locally diffused cell (PERL) which leads to the improvement in efficiency of cell due to an increase in V_{OC} [5-6].

Moreover, bifacial cells with use of a passivated diffused carrier collector and a printed Al/Ag or Cu plated grid on both sides of the device is used to achieve 700 mV V_{OC} developed by ECN [7]and Technologies developed by Stanford university to avoid front metal shading losses, where both carriers

Collectors are located at the back side of the cell, with 24% efficiency [9-12].

TetraSun [8]. Furthermore, interdigitated Back Contacts (IBC) are another class of solar cell

In addition, considering super heterojunction (SHJ) cells, high V_{OC} (more than 730mV) and better surface passivation are obtained by depositing thin layers of a-Si (amorphous Si) on both sides of the cell. Finally, a transparent Indium Tin Oxide (ITO) layer is used at the front surface which serves as an antireflection coating, while making a good ohmic contact [13-15].

The texturing process enables morelight trapping and produces significant gain in solar cell performance especially for solar cells made with relatively weak absorbing semiconductors, such as crystalline silicon and amorphous silicon–hydrogen alloys [16-18]. Various geometries are suggested for maximum light trapping achievement, such as: plasmonic light trapping [19-20] periodic hexagonally symmetric ‘‘honeycomb’’ surface texture [21], photonic crystal intermediate reflector [22] and modulated surface texture [23]. The above mentioned textures reduce reflection loss as well as substantially increase in the cell's effective optical thickness by causing light to be trapped within the cell by total internal reflection [24].

In this paper a monocrystalline Si solar cell is optimized by considering main process parameters in the design process. The optimization is performed by numerical simulation and analytical equations for the performance parameters of the solar cell. Section II introduces the main structure which is optimized in this paper and the theory for

[1] Ph.D. Student, Department of Electrical Engineering, Iran, University of Science and Technology,Tehran, Iran h-bashiri@elec.iust.ac.ir

[2] Corresponding Author: Assistant Professor, Department of Electrical Engineering, Iran University of Science and Technology, Tehran, Iran, karami@iust.ac.ir

[3] Professor, Department of Electrical Engineering, Iran University of Science and Technology, Tehran, Iran, shahramm@iust.ac.ir

its evaluation. In section III the optimization is categorized in 3 different branches: surface texture, substrate thickness, and the doping concentrations. Moreover, the final structure is characterized in the mentioned chapter, while the conclusions are given in sectionIV.

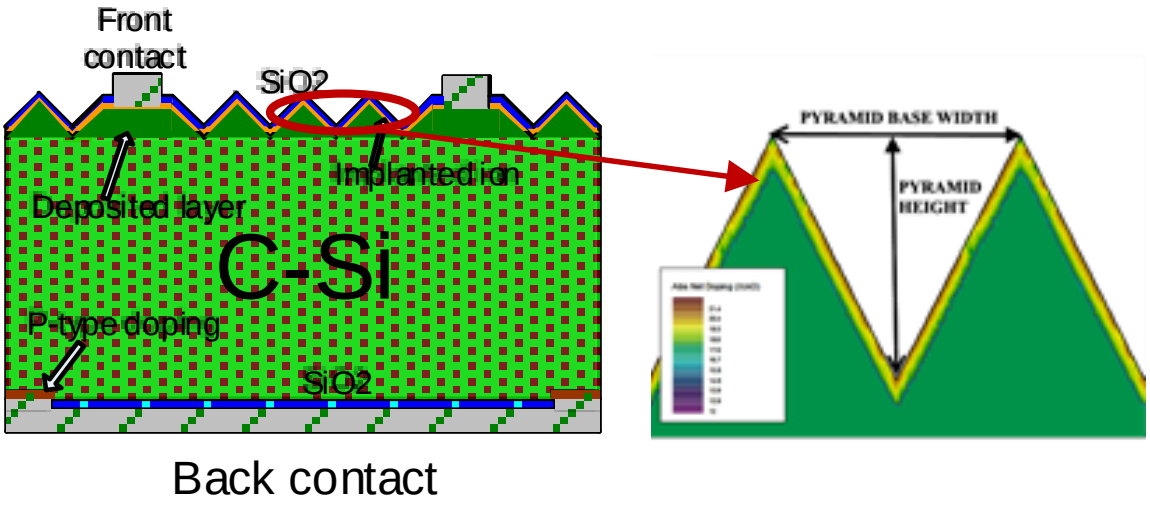

Fig. 1. Solar cell cross section using inverted pyramid for efficiency enhancement.

II.SOLAR CELL STRUCTURE & THEORY

Figure 1 shows the solar cell cross section analyzed and optimized in this paper. Inverted pyramid texture has proven maximum light trapping for monocrystalline silicon solar cell [22,24]. The simulation is performed by a commercially available device simulator [25]. A p-type <100> oriented single crystalline silicon with 55µm thickness is used as the substrate and inverted pyramids are created by the etching process. Different procedures can be used to obtain inverted pyramid structure with different slopes and aspect ratios for example reactive ion etching [26], nanoimprint lithography [27] and femtosecond laser structuration [28]. The phosphorous atoms are implanted on surface of etched silicon layer to form the cathode part of the photodiode. The implantation process is followed by 30 minutes' drive-in and annealing process at 1050oC.

After p-n junction formation, a thin SiO2 layer is thermally grown. This layer increases VOC, improves collection probability of photogenerated carrier near the surface and also acts as an antireflection layer [18]. The final step in implementation process is etching, metallization and contact formation. Again, a thin film of thermally grown SiO_2 layer on the back surface of c-Si wafer is used to increase the internal reflection. The generated photocurrent illuminated under the short circuit biasing condition is proportional to the incident spectrum and the cell's external quantum efficiency (EQE). The short circuit current is [29-34]:

$$J_{sc} = q \int b(E) EQE(E)\, dE \qquad (1)$$

Where $b(E)$ is the incident spectrum between E and $E+dE$ and q is the charge of electron. When a forward bias is applied across a solar cell, dark current (J_{dark}), which is in the opposite direction of the photocurrent created by potential difference between the front and rear contacts. The dark current density is [29-34]:

$$J_{dark} = J_0 \left(e^{\frac{qV}{k_B T}} - 1 \right) \qquad (2)$$

Where J_0 is dark current saturation density and is proportional to the total recombination in the device, V is the electrostatic potential across the device, k_B is the Boltzmann's constant and T is the temperature in Kelvin. The total current can then be approximated as the sum of the dark current and the photocurrent:

$$J_{tot} = J_{sc} - J_{dark} \qquad (3)$$

By definition, under open circuit condition the total current in the device is zero, therefore, we can define the o V_{OC} as the voltage at which J_{dark} and J_{SC} are equal. An Expression for V_{OC} can be derived from equations 2 and 3 by substituting 0 for J_{tot}, Voc for V, and solving for Voc which can be expressed as [29-34]:

$$V_{oc} = \frac{k_B T}{q} ln \left(\frac{J_{sc}}{J_0} - 1 \right) \qquad (4)$$

Since the power density function $P = J(V).V$ has only 1 optimum the voltage at maximum

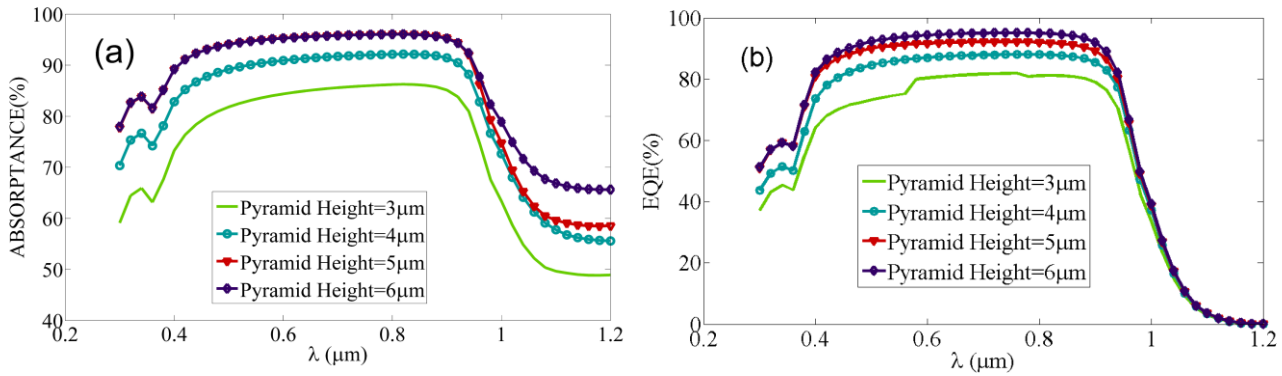

Fig. 2. (a) Absorbance and (b) EQE of simulated structure as a function of wavelengt

Power point V_{mpp} can be obtained by solving $\frac{dJ(V).V}{dV} = 0$,

The FF can be calculated with $J_{mpp} = J(V_{mpp})$ [33,34]

$$FF = \frac{J_{mpp}.V_{mpp}}{J_{sc}.V_{oc}} \quad (5)$$

The conversion efficiency is the ratio of the maximum output power to the incident power [33, 34]:

$$EFF = \frac{J_{mpp}.V_{mpp}}{P_{in}} \quad (6)$$

The External Quantum Efficiency (EQE) for p-n junction device under illumination calculated by [29-34]:

$$EQE = \frac{J(\lambda)}{qF_0(\lambda)\big(1 - R(\lambda)\big)} \quad (7)$$

Where $F_0(\lambda)$is incident photon density per wavelength interval, $R(\lambda)$ is reflection coefficient at the surface and $J(\lambda) = J_{ph} = J_p + J_n + J_{dep}$ is generated current in p-layer, n-layer and depletion region. Lambertian scattering model can use to describe absorbed light by trapping structures however it is possible to obtain more absorption with semi-regular geometries for textured surface [35]:

$$A = \frac{1 - e^{(-2\alpha W_{op})}}{1 - \left(1 - \frac{1}{n^2}\right) e^{(-2\alpha W_{op})}} \quad (8)$$

Where $W_{op} = W\frac{2+a(\alpha W)^b}{1+a(\alpha W)^b}$, w is absorber layer thickness, a = 0.935 and b = 0.67, α is silicon absorption coefficient and n is silicon refractive index [36]:

$$J_{sc} = f_c q \int_0^{\infty} \phi(\lambda) A(\lambda) d\lambda \quad (9)$$

Where f_c is carrier collection probability.

III. OPTIMIZATION

Absorption is defined as the fraction of absorbed light to total incident solar irradiance. Increasing the absorption will lead to the overall increase in the solar cell efficiency. Absorption can be derived from reflection and transmission measurements, and can be affected by surface texture and solar cell's thickness [11, 15].

a) Surface texture effect

Texturing in solar cell's surface is a technique to increase the number of absorbed photons thereby by equation (7) it cause to increase the J_{SC}. This is due to reduction in reflections, multiple attempts at transmission through the front surface and longer path lengths for scattered light at angles that lead to improve solar cell's efficiency. The shape and dimension of surface texture play a critical role in enhancing the light trapping [35]. In this part pyramid texture dimension effect in the optical absorption is studied. The thickness of active layer set 100 μm and 10μm is regarded as the base of inverted pyramid and different pyramid heights are examined to extract the maximum efficiency.the simulation is performed under beam intensity of b=1000 W/m^2, the substrate doping of 10^{17} atoms/cm^3, phosphorous ion-implanted concentration doping of 10^{18} atoms/cm^3. Here, the region underlying anode Contact should be heavily p-doped to prevent the schottky contact formation and reduce minority carrier recombination near the

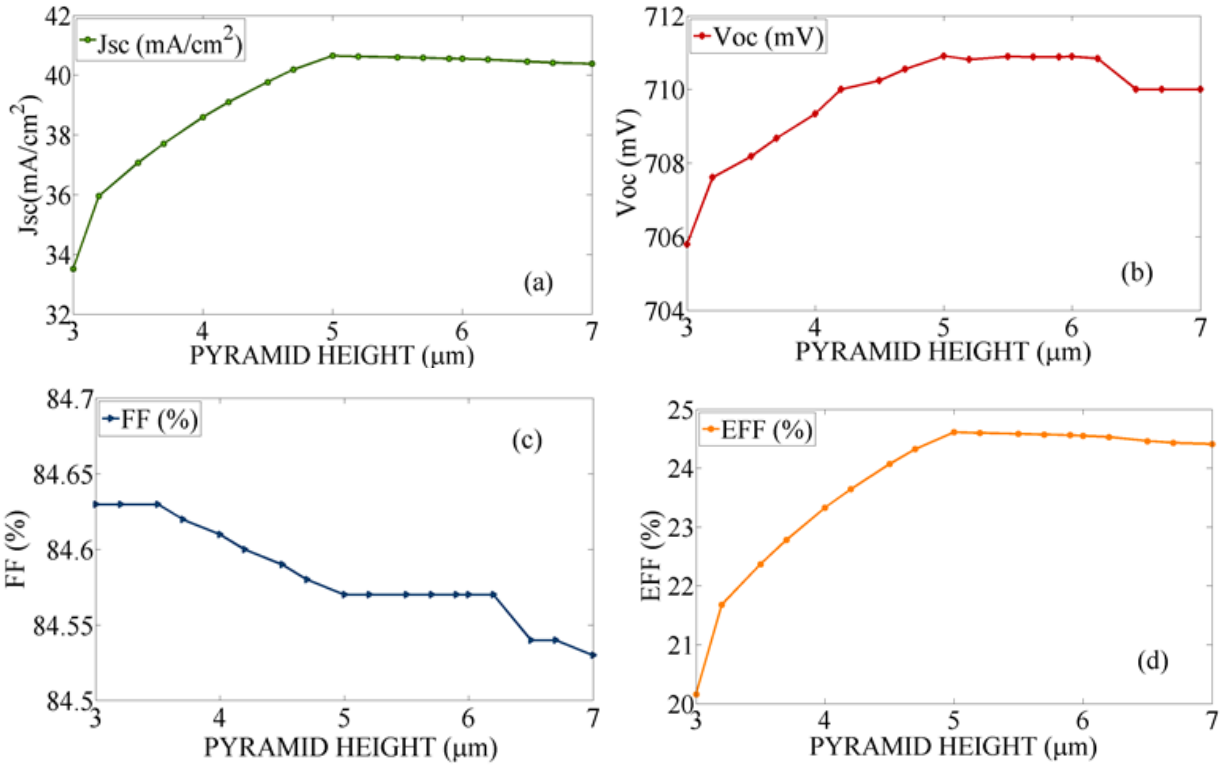

Fig. 3. Solar cell's main parameters as a function of Pyramid height: a) 6 mA increase in J_{SC}, b) 5mV increase in V_{OC} , c) 0.1% reduce in *FF* and d) more than 4.5% increase in efficiency, resulted due to increase in light absorption by increasing height from 3 to 5μm.

contact. Fig 2 shows different inverted pyramid height effect on The solar cell absorption and external quantum efficiency (EQE). It is obvious that increasing the solar cell's height from 3 to 5 μm leads to considerable increase in absorbed light fraction and corresponding EQE. Increasing photon absorption rate in lower wavelength (high-energy photons) is more than photons with wavelength about 900nm when the pyramid height increase from 3 to 5 μm. the increasing absorption rate is due to more effective light trapping for photons with lower wavelength. this high rate increasing in absorption rate is due to more effective light trapping for photons with lower wavelength. Moreover, the results show an increase in absorption in the whole spectral range from 300 to 1200 nm when the inverted pyramid height increases from 3 to 5 μm. Further increasing in the pyramid height, only affects high wavelength absorption. Moreover, maximum external quantum efficiency EQE~ 93% is achieved in spectral wavelength from 400 to 950 nm when the height is set to 6 μm. Fig 3 shows the effect of increasing light Considering pyramid height and base width 5 µm and 10 µm respectively, Fig 4 shows the effect of Si substrate thickness on absorbed light fraction and absorption on solar cell's main figures of merit. The J_{SC} increases from 33.5 mA/cm^2 to 40.65 mA/cm^2 when the height increases from 3 to 5μm, more increasing in pyramid height lead to J_{SC} decreases slightly because the effect of parasitic electrical resistance is dominant on light absorption increasing in high wavelength. Moreover, V_{OC} increases slightly when inverted pyramid height increases from 3 to 5μm and then drops. This phenomenon is due to inter-relation between V_{OC} and J_{SC} (eq. 4). Increasing inverted pyramid height leads to a decrease in *FF* due to an increase in electric resistance [37]. Changes of V_{OC} and *FF* is only 5mV and 0.2% respectively for inverted pyramid height variation from 3 to 7 μm and so the efficiency behave like J_{SC} changes. This study shows that the optimum inverted pyramid height value to achieve maximum efficiency is about 5μm.

b) Substrate thickness effect

Increasing solar cell thickness lead to increase in absorbed light fraction, EQE, short circuit current density [29-34] and consequently increase solar cell's efficiency according to equation (9) With EQE in spectral wavelength from 300nm to 1200nm. It can be seen that 90% of photons with

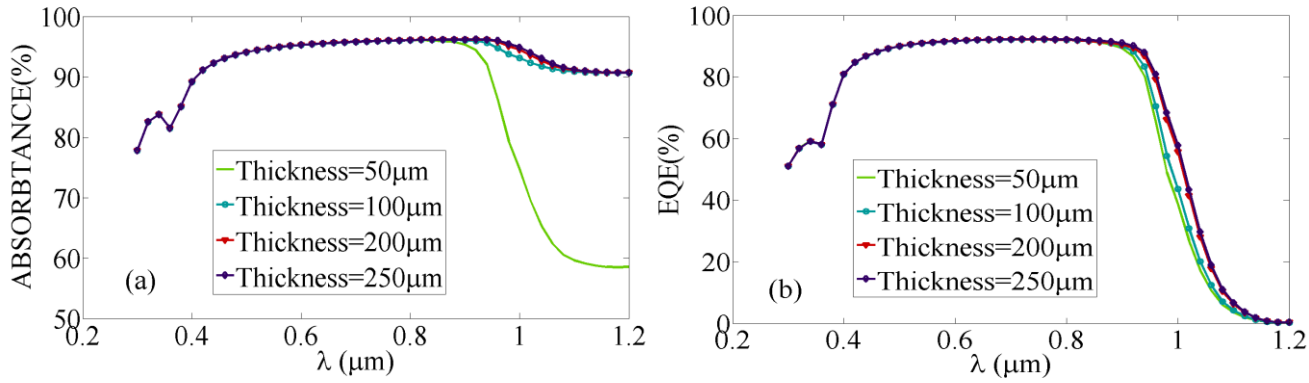

Fig. 4. (a) Absorptance and (b) EQE of simulated structure as a function of solar cell's thickness

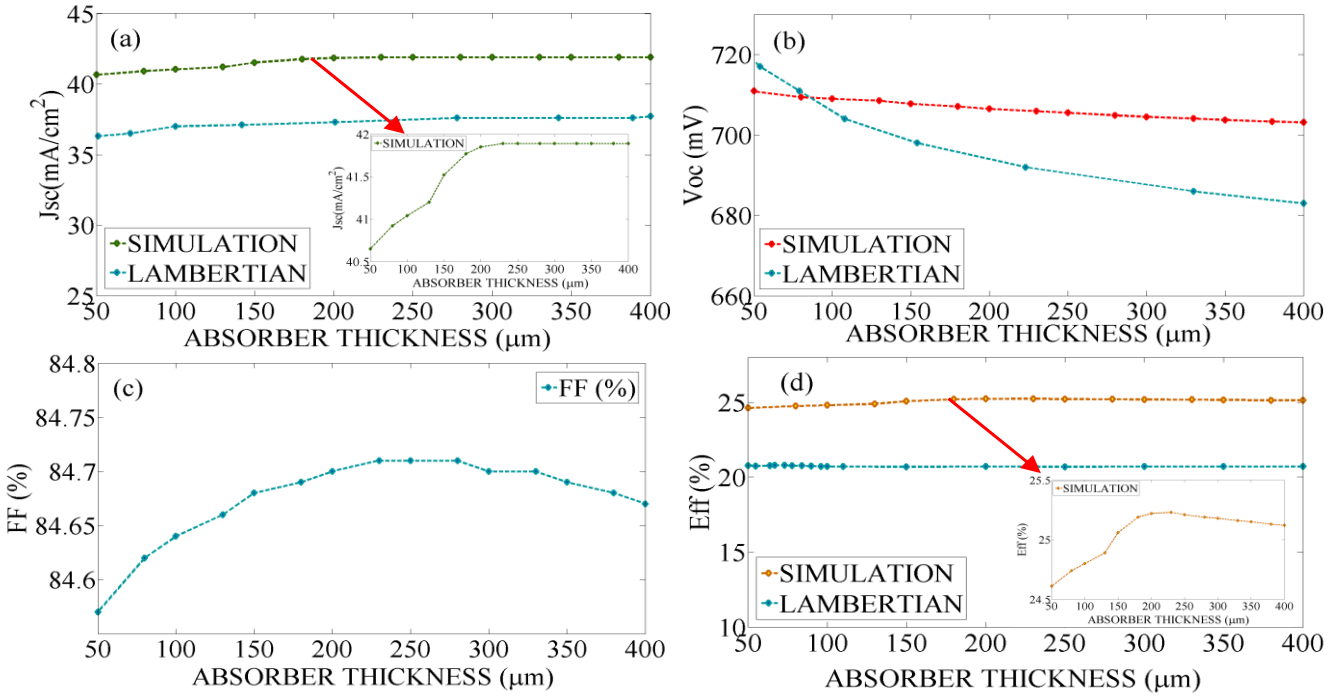

Fig. 5. solar cell's main parameters as a function of substrate thickness: a) 1.4 mA increase in J_{SC}, b) 0.12% increase in *FF*, c) 4mV reduce in V_{OC} and d) 0.6% increase in efficiency is resulted, when thickness increases from 50 to 200μm.

wavelength smaller than 900 nm absorbed in the 50μm top of the substrate.

Increasing solar cell's absorber thickness will lead to increasing absorption and EQE of high wavelength photons. More than 250 μm substrate thickness does not change the solar cell's efficiency significantly, since a small portion of sun's long wavelength photons are absorbed in the thicknesses after 250 μm [34].

Fig 5 shows the effect of c-Si absorber thickness on solar cell's parameters, as shown in small thickness of the c-Si absorber dependent of the J_{SC} on the thickness is considerable and it start to saturate at around 200 μm that correspond with absorbed light in different thickness, in thick c-Si absorber, if the effect of bulk recombination and surface recombination suppressed by high quality c-Si ($\tau > 10^{-4}$ s) and good passivation (S_n <*0.1 m/s*) V_{OC} Only slightly dependent on the thickness of the c-Si absorber. Simulation result show that when the absorber thickness increase from 50 to 400 μm the V_{OC} decreases slightly from 711 to 703 mV because the electrical parasitic resistance increases. As shown we can realize that 200-250μm is optimum absorber thickness for achieve The best efficiency conversion and about 84.7% *FF*.

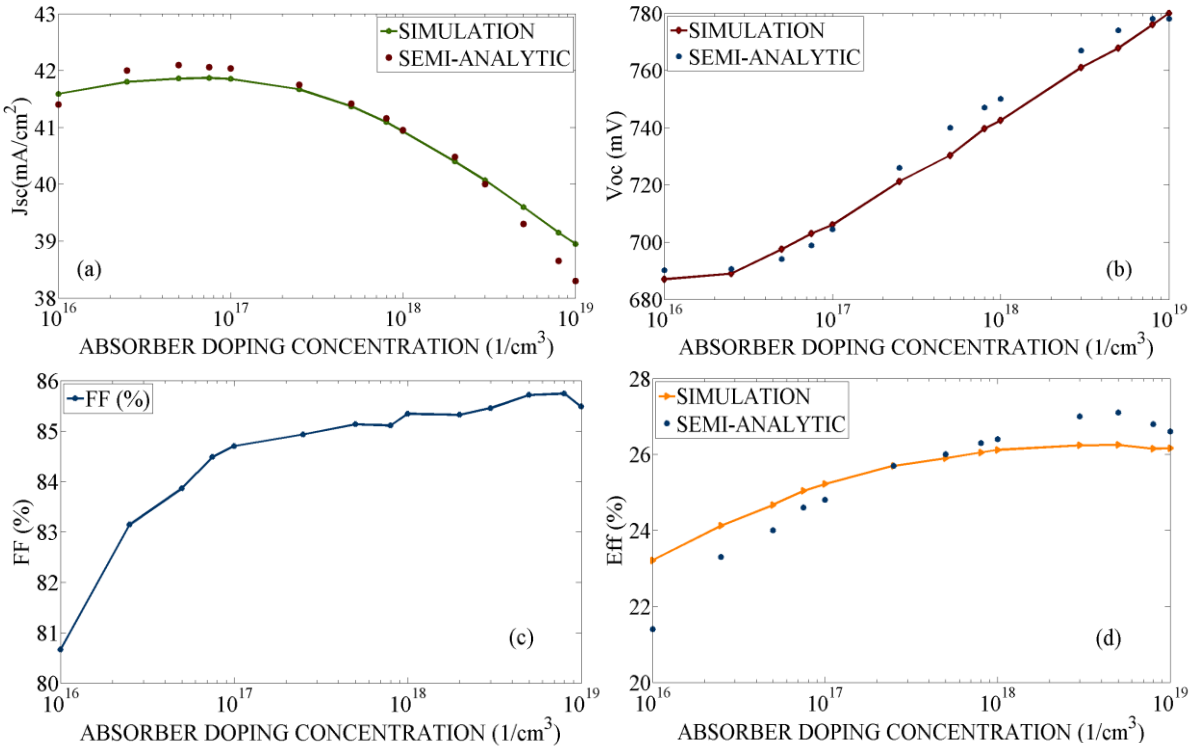

Fig. 6. The effect of c-Si absorber doping on solar cell's parameters: a) short circuit current, b) open circuit voltage, c)Fill Factor and d) Efficiency

c) Doping concentration optimization

As mentioned in previous section recombination losses are inversely proportional to the minority carrier lifetime (τ) which the latter depends on doping concentration of c-Si absorber. So N_A increase led to increase in V_{OC}. because the dark saturation current densities J_0 decreases by [38,39]:

$$J_0 = \frac{qR}{(n_0+\Delta n)(p_0+\Delta n)/n_i^2-1} \quad (10)$$

where R is local recombination rate at metal interface and bulk, n_0 is the electron equilibrium carrier concentration, p_0 is hole carrier concentration, n_i is intrinsic silicon carrier concentration and Δn is local excess carrier densities in various cell regions and calculated by [40]:

$$\Delta n = (n_0 + p_0)\left(\sqrt{1 + \left(2n_i/(n_0 + p_0)\right)^2 e^{qV_{oc}/kT}} - 1\right)/2 \quad (11)$$

In bulk $p_0 \approx N_A$ and $p_0 + n_0 \approx N_A$, hence equation (11) can be rewritten as:

$$\Delta n = N_A\left(\sqrt{1 + \left(2n_i/(N_A)\right)^2 e^{qV_{oc}/kT}} - 1\right)/2 \quad (12)$$

To optimize doping concentration of c-Si absorber region, absorber thickness set to 200μm, pyramid height and pyramid base width set to 5-µm and 10-µm respectively and N_A varies from 1×10^{16} (cm^{-3}) to1×10^{19} (cm^{-3}) . Recombination losses decrease J_{SC} and doping concentration changes cell electrical resistivity that directly affect FF. Also doping concentration mainly affects V_{OC}; therefore, to achieve the best conversion efficiency, there is a tradeoff between electrical resistivity and recombination losses in bulk thickness of c-Si absorber.

In this paper, Semi-analytic method is used to obtain exact solution for solar cell's parameters versus doping concentration. In this method, an initial value for V_{OC} and J_{SC} is guessed, then Δn and J_0 are calculated, V_{OC} and J_{SC} are updated afterwards. These processes repeat to V_{OC} and J_{SC} values converge.

Fig. 6 shows the absorber doping concentration effect on V_{OC}, J_{SC}, FF, and conversion efficiency Eff. As shown J_{SC} start to increase at the beginnin

Till 41.7 mA/cm^2 at $N_A = 1 \times 10^{17}$ (cm^{-3}) because the effect of electrical resistivity decreasing is dominant on recombination losses and then linearly drop down.

The *FF* increase from 80.7% to more than 85%, *Eff* behave to increase first and slightly drop for doping concentration more than 5×10^{18} (cm^{-3}), because J_{SC} decreasing by recombination losses is dominant factor, maximum efficiency obtained 26.27% at c-Si absorber doping concentration 3×10^{18} (cm^{-3}). Simulation results are in agreement with the semi-analytic results.

The final structure has 200μm absorber thickness and 5μm inverted pyramid height when the base width of inverted pyramid set 10μm lead to optimum light absorption obtained. The doping concentration is N_A =1×10^{17} (cm^{-3}), N_D =5×10^{17} (cm^{-3}), N_A =3×10^{18} (cm^{-3}) in p-deposited layer, ion-implanted phosphor and absorber layer respectively on this optimum structure lead to best conversion efficiency 26.3% with J_{SC}~ 40.07 mA/cm^2, V_{OC} =761 mV, and fill factor~85.3%, obtained the illuminated *IV* curves of the optimized cells are shown in Fig. 7, and the detailed cell figure of merits are given in Table I.

Table I. Comprasion with other work

Reference	V_{OC} (mV)	J_{SC} (mA/cm^2)	*FF* (%)	Eff (%)
[40]	646	44.4	83.66	24.01
[41]	721	40.46	82.9	24.2
[22]	696	42	83.6	24.4
[4]	706	42.7	82.8	24.7
Present work	761	40.07	85.34	26.27

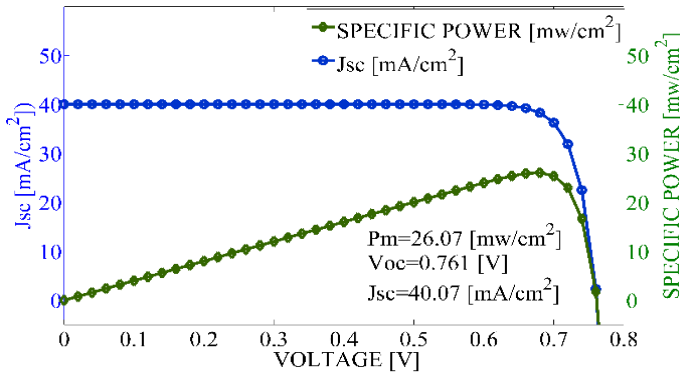

Fig. 7. resulted J-V and P curve under illumination

IV. CONCLUSION

A monocrystalline p-type Si solar cell with use of thin film thermally grown SiO_2 layer on surfaces and with the inverted pyramid texture has been studied through numerical simulations. To achieve the best conversion efficiency, the optimum value for geometrical dimensions, doping concentrations, and absorber layer thickness are calculated. In conclusion, the high V_{OC} of 761mV, 40.07 mA/cm^2 J_{SC}, 85.4% fill factor and 26.3% conversion efficiency is achieved. To the best of our knowledge this work presents the maximum conversion efficiency for mono-crystalline Si solar cells in compare with the state of the art works.

References

[1] M. A. Green, K. Emery, Y. Hishikawa, W. Warta, and E. D. Dunlop, "Solar cell efficiency tables (version 39)," Progress Photovoltaics: Res. Appl., vol. 20, no. 1, pp. 12–20, 2012.

[2] Z. Wang, P. Han, H. Lu, H. Qian, L. Chen, Q. Meng et al., "Advanced PERC and PERL production cells with 20.3% record efficiency for standard commercial p-type silicon wafers," Prog. Photovoltaics, Res. Appl., vol. 20, pp. 260–268, 2012.

[3] M. A. Green, "Limits on the open-circuit voltage and efficiency of silicon solar cells imposed by intrinsic Auger processes," IEEE Trans.Electron Devices, vol. ED-31, no. 5, pp. 671–678, May 1984.

[4] M. A. Green, "The path to 25% silicon solar cell efficiency: History of silicon cell evolution," Prog. Photovoltaics, Res. Appl., vol. 17, pp. 183–189, 2009.

[5] A. Wang, J. Zhao, and M. A. Green, "24% efficient silicon solar cells," Applied Physics Letters, vol. 57, no. 6, pp. 602–604, 1990.

[6] S. W. Glunz, J. Benick, D. Biro, M. Bivour, M. Hermle, D. Pysch, M.Rauer, C. Reichel, A. Richter, M. Rudiger, C. Schmiga, D. Suwito, A. Wolf, and R. Preu, "n-type silicon - enabling efficiencies >20% in industrial production," 35th IEEE Photovoltaic Specialists Conference (PVSC), 2010, pp. 50–56.

[7] I. G. Romijn, B. van Aken, J. Anker, A. R. Burgers, A. Gutjahr, B.Heurtault, M. Koppes, E. Kossen, M. Lamers, D. S. Saynova, C. J. J. Tool, Lang Fang, Xiong Jingfeng, Li Gaofei, Xu Zhuo, Wang Hongfang, Hu Zhiyan, P. R. Venema, and A. H. G. Vlooswijk, "Industrial Implementation of Efficiency Improvements in N-type Solar Cells and Modules," in 27th European Photovoltaic Solar Energy Conference and Exhibition, 24-28 Sept. 2012, pp. 533–7.

[8] O. Schultz-Wittmann, D. De Ceuster, A. Turner, D. Crafts, R. Ong, D.

Suwito, L. Pavani, and B. Eggleston, "Fine line copper based metallization for high efficiency crystalline silicon solar cells," 27th European Photovoltaic Solar Energy Conference and Exhibition, 24-28 Sept. 2012, pp. 596–9.

[9] A. Lennon, Y. Yao, and S. Wenham, "Evolution of metal plating for silicon solar cell metallisation, Progress in Photovoltaics: Research and Applications," vol. 21, no. 7, pp. 1454–1468, 2013.

[10] M. D. Lammert and R. J. Schwartz, "The interdigitated back contact solar cell: A silicon solar cell for use in concentrated sunlight," IEEE Transactions on Electron Devices, vol. 24, no. 4, pp. 337–342, 1977.

[11] R. M. Swanson, S. K. Beckwith, R. A. Crane, W. D. Eades, Y. H. Kwark, R. A. Sinton, and S. E. Swirhun, "Point-contact silicon solar cells," IEEE Transactions on Electron Devices, vol. 31, no. 5, pp.661–664, 1984.

[12] D. D. Smith, P. J. Cousins, A. Masad, A. Waldhauer, S. Westerberg, M. Johnson, X. Tu, T. Dennis, G. Harley, G. Solomon, S. Rim, M. Shepherd, S. Harrington, M. Defensor, A. Leygo, P. Tomada, J. Wu, T. Pass, L. Ann, L. Smith, N. Bergstrom, C. Nicdao, P. Tipones, and D. Vicente, "Generation III high efficiency lower cost technology: Transition to full scale manufacturing," 38th IEEE Photovoltaic Specialists Conference (PVSC), 2012, pp. 1594–001597.

[13] M. Taguchi, A. Yano, S. Tohoda, K. Matsuyama, Y. Nakamura, T. Nishiwaki, K. Fujita, and E. Maruyama, "24.7 % Record Efficiency HIT Solar Cell on Thin Silicon Wafer," IEEE Journal of Photovoltaics, 1, pp. 7–15, Jan.2012.

[14] T. Kinoshita, D. Fujishima, A. Yano, A. Ogane, S. Tohoda, K. Matsuyama, Y.Nakamura, N. Tokuoka, H. Kanno, H. Sakata, M. Taguchi and E. Maruyama, "the Approaches for High Efficiency HIT TM Solar Cell with Very Thin (<100μm) Silicon Wafer over 23%," 26th European Photovoltaic Solar Energy Conference and Exhibition, p. 871, Hamburg, Germany, September 2011

[15] K. Maki, D. Fujishima, H. Inoue, Y. Tsunomura, T. Asaumi, S.Taira,T. Kinoshita, M. Taguchi, H. Sakata, H. Kanno, and E.Maruyama,"Highefficiency HIT solar cells with a very thin structure enabling a high VOC," presented at the 37th IEEE Photovoltaic Specialists Conf., Seattle, WA, USA, 2011.

[16] M. Taguchi, A. Yano, S. Tohoda, K. Matsuyama, Y. Nakamura, T. Nishiwaki, K. Fujita, and E. Maruyama, "24.7% record Efficiency HIT solar cell on thin silicon wafer," *IEEE J. Photovolt.*, vol. 4, no. 1, pp. 96–99, Jan. 2014.

[17] Z. C. Holman, A. Descoeudres, L. Barraud, F. Z. Fernandez, J. P. Seif, S. De Wolf, and C. Ballif, "Current losses at the front of silicon heterojunction solar cells," *IEEE J. Photovolt.*, vol. 2, no. 1, pp. 7–15, Jan.2012.

[18] M.W.M.Van Cleef, F.A. Rubinelli, J. Daey Ouwens, and R. E. I. Schropp, "Amorphous-crystalline heterojunction silicon solar cells with an a-SiC:H window layer," in *Proc. 19th Eur.Photovoltaic Sol. Energy Conf.*, Nice, France, 1995, pp. 1303–1306.

[19] H. Tan, R.Santbergen, H.M.Smets, M.Zeman, "Plasmonic light trapping in thin- film silicon solar cells with improved self-assembled silver nanoparticles," Nano Lett. 12(2012)4070–4076.

[20] H.Tan, L.Sivec, B.Yan, R.Sentbergen, M.Zeman, H.M.Smets, "Improved light trapping in micro crystalline silicon solar cells by plasmonic back reflector with broad angular scattering and low parasitic absorption," Appl.Phys. Lett.102 (2013)153902.

[21] J. Upping, A.Bielawny, R.B.Wehrspohn, T.Beckers, R.Carius, U.Rau, S.Fahr, C.Rockstuhl, F.Lederer, M.Kroll, T.Pertsch, L.Steidl, R.Zentel, "Three-dimensional photonic crystalline intermediate reflectors for enhanced light trapping in tandem solar cells," Adv.Mater, 23(2011) 3896–3900.

[22] J. Zhao, A.Wang, M. A. Green, and F. Ferrazza, "19.8% efficient 'honeycomb' textured multicry stalline and 24.4% monocrystalline silicon solar cells," *Appl. Phys. Lett.*, vol. 73, pp. 1991–1993, 1998.

[23] O. Isabella, J.Krc, M.Zeman,"Modulated surface textures for enhanced light- trapping in thin-film silicon solar cells," Appl. Phys. Lett. 97 (2010)

[24] L. Zhao, C. L. Zhou, H. L. Li, H. W. Diao, and W. J. Wang, "Design Optimization of bifacial HIT solar cells on p-type silicon substrates by Simulation," *Solar Energy Mater. Solar Cells*, vol. 92, pp. 673–681, Jun. 2008

[25] Atlas, Athena and Devedit user's www.silvaco.com

[26] Razykov, T.Ferekides, C.Morel, D.Stefanakos, E.Ullal, H.Up adhyaya, H. 2011, "Solar photovoltaic electricity: current status and future prospect," Sol. Energy 85 (8), 1580-1608.

[27] Yu, Z., Gao, H., Wu, W., Ge, H., Chou, S.Y., 2003, "Fabrication of large area subwavelength antireflection structures on Si using tri layer resist nanoimprint lithography and liftoff," J. Vac. Sci. Technol. B: Micro electron. Nanometer Struct. 21 (6), 2874-2877.

[28] Crouch, C.H., Carey, J.E., Warrender, J.M., Aziz, M.J., Mazur, E., Gnin, F.Y., 2004, "Comparison of structure and properties of Femtosecond and nanosecond laser-structured silicon", Appl. Phys. Lett. 84 (11), 1850-1852.

[29] Law, M.E.et. al, "Self-Consistent Model of Minority-Carrier Lifetime, Diffusion Length, and Mobility", IEEE Electron Device Letters Vol. 12, No. 8, 1991.

[30] Roulston, D.J., N.D. Arora, and S.G. Chamberlain, "Modeling and Measurement of Minority-Carrier Lifetime versus Doping in Diffused Layers of n ±p Silicon Diodes", IEEE Trans. Electron Devices Vol. 29 (Feb. 1982): 284-291.

[31] J.C. Mifiano, A. Luque, "Geometrical patterns producing almost isotropical light confinement," Eighth EC Photovoltaic Solar Energy Conference: Proceedings of International Conference Held at Florence, Italy, 9-13 May 1988, 1988.

[32] M. A. Green, "Solar cells: Operating principles, technology, and system Applications", Englewood Cli_s, NJ, Prentice-Hall, Inc., 1982.~288 p., 1982).

[33] K. R. Mcintosh, Lumps, Humps and Bumps: Three Detrimental E ects in the Current Voltage Curve of Silicon Solar Cells, PhD thesis UNSW 2001.

[34] A. Luque and S. Hegedus, Handbook of Photovoltaic Science and Engineering (Wiley, 2010).

[35] M. A. Green, "Lambertian light trapping in textured solar cells and lightemitting diodes: Analytical solutions," *Prog. Photovoltaics: Res.* Appl, vol. 10, pp. 235–241, 2002.

[36] Thomas P. White, Niraj N. Lal, and Kylie R. Catchpole, "Tandem Solar Cells Based on High-Efficiency c-Si Bottom Cells: Top Cell Requirements for >30% Efficiency", IEEE JOURNAL OF PHOTOVOLTAICS, VOL. 4, NO. 1, JANUARY 2 2014

[37] Ankit Khanna, Thomas Mueller, Rolf A. Stangl, Bram Hoex, Prabir K. Basu, and Armin G. Aberle, "A Fill Factor Loss Analysis Method for Silicon Wafer Solar Cells", IEEE JOURNAL OF PHOTOVOLTAICS, VOL. 3, NO. 4, OCTOBER 2013

[38] Fossum, J.G. and D.S. Lee, "A Physical Model for the Dependence of Carrier Lifetime on Doping Nondegenerate Silicon", Solid State Electronics Vol. 25 (1982): 741-747.

[39] Antoine Descoeudres, Zachary C. Holman, Loris Barraud, Sophie Morel, Stefaan De Wolf, and Christophe Ballif, ">21% Efficient Silicon Heterojunction Solar Cells on n- and p-Type Wafers Compared," IEEE JOURNAL OF PHOTOVOLTAICS, VOL. 3, NO. 1, JANUARY 2013

[40] N. Dasgupta and A. Dasgupta, "Semiconductors" in *Semiconductor Devices*. New Delhi, India: Prentice-Hall, 2004.

[41] P. J. Cousins, D. D. Smith, H-C. Luan, J. Manning, T. D. Dennis, A.Waldhauer, K. A. Wilson, G. Hartley, and W.P.Mulligan, "Generation3: Improved performance at lower cost," in Proc.33rd IEEE Photovoltaic Spec. Conf., 2010, pp. 275–278.

[42] William R. Taube, A. Kumar, "Simulation and optimization of N-type PERL silicon solar cell structure" J. Nano-Electron. Phys.3 (2011) No1, pp. 1127-113